

## Physical Gelation of Amorphous Polymers in a Mixture of Solvent and Nonsolvent

S.-G. Li, Th. van den Boomgaard,\* C. A. Smolders, and H. Strathmann

Department of Chemical Technology, University of Twente, P.O. Box 217,  
7500 AE Enschede, The Netherlands

Received June 26, 1995; Revised Manuscript Received December 2, 1995<sup>®</sup>

**ABSTRACT:** The formation of phase inversion membranes made by immersion precipitation from a ternary system consisting of an amorphous polymer, a solvent, and a nonsolvent has been rationalized by assuming a gelation process. The treatise is based on a hypothesis developed by Berghmans for a binary system consisting of a polymer and a solvent. The ternary phase diagram for the mixture of H<sub>2</sub>O–NMP (*N*-methylpyrrolidone)–PES (poly(ether sulfone)) was determined at 25 °C. In this system three boundaries could be identified, i.e., a vitrification, a gelation, and a binodal boundary. It was found that for this system and a system composed of H<sub>2</sub>O–DMAC (*N,N*-dimethylacetamide)–PSF (polysulfone), vitrification is the only mechanism responsible for the structure fixation of membranes prepared by liquid–liquid demixing due to immersion precipitation. For the system of MPD (2-methyl-2,4-pentanediol)–NMP–PES, it was found that a membrane can be formed by vitrification as a result of immersion precipitation prior to liquid–liquid demixing. The depressions of the glass transition temperature of PES by the addition of FP (*N*-formylpiperidine), DMSO (dimethyl sulfoxide), DMAC, or NMP as well as by a mixture of NMP and water are determined.

### Introduction

Gelation is often considered as the mechanism leading to skin formation of membranes prepared by immersion precipitation.<sup>1–3</sup> It has been suggested that gelation suppresses liquid–liquid demixing due to kinetic hindering caused by the high viscosity of a gelled polymer solution in the skin of the membrane.<sup>1–3</sup> However, this hypothesis has never been proven experimentally.

Conventionally a gel is defined as a highly viscous, coherent, soft, and elastic structure that contains predominantly liquid.<sup>4</sup> Gels are characterized by a loose three-dimensional network and cover a wide spectrum of structures from homogeneous solutions (where entropy of the mixture is the main factor responsible for maintaining the liquid) to a heterogeneous rigid porous system (where capillary forces are responsible for maintaining the liquid).<sup>5</sup> A gel is created by the formation of connecting elements (junctions) in the initial liquid. These junctions can be formed either by chemical cross-links or by physical associations. Chemical cross-linking, i.e., covalent binding of polymer chains by means of a chemical reaction, is unlikely to occur during formation of phase inversion membranes. In case that physical associations are responsible for gel formation, the process is thermally reversible and is referred to as thermoreversible or physical gelation.

Recently theoretical progress has been made for the description of the thermodynamic properties of reversible gels whose junctions are formed by the clustering of associating groups.<sup>6,7</sup> Tanaka and Stockmayer extended this theoretical work to study the interference between gelation and liquid–liquid phase separation.<sup>8</sup> They showed that there is indeed competition between gelation and phase separation for a polydisperse polymer in a solvent, a pseudobinary system. In their opinion those theoretical results are applicable to real systems; however, no experimental evidence has been given yet.

In practice the mechanism for physical gelation is system-dependent.<sup>9,10</sup> For semicrystalline polymers, it

is often found that gelation is initiated by the formation of microcrystallites, i.e., localized interchain crystallization.<sup>9,12–14</sup> These microcrystallites connect various polymeric chains and form a three-dimensional network. The formation of the microcrystallites is time-dependent. Matsuo et al. stressed the point that inhomogeneities of such a well-defined gel affect its physical properties, among others, the permeability. Using light scattering they studied the origin of these inhomogeneities which are partly present at the onset of the gelation process.<sup>15</sup>

For membrane formation, at least a pseudoternary system has to be used, in which often semicrystalline polymers are applied. Due to the fact that membrane formation is generally a fast process, only polymers that are capable of crystallizing rapidly, such as polyethylene, polypropylene, aliphatic polyamides, etc., will exhibit an appreciable amount of crystallinity during phase inversion.<sup>14</sup> Other semicrystalline polymers, such as poly(2,6-dimethyl-1,4-phenylene oxide) (PPO), contain low to very low crystallinity in the formed membranes, although they are capable of forming gels initiated by crystallization in various solvents.<sup>16</sup> Considering the fact that the skin of a membrane is formed in a very short time, i.e., in a few seconds or less, it is unlikely that any crystallinity exists in the skin of most membranes.<sup>17</sup> Apparently, gelation by means of crystallization cannot be regarded as a general scheme for skin formation. Other means of gelation such as the formation of hydrogen bonding<sup>18</sup> are very slow processes and are even less likely to occur during membrane skin formation.<sup>19</sup>

Gelation can also take place in solutions of amorphous polymers, such as atactic polystyrene (aPS).<sup>20–23</sup> Gelation in amorphous polymer can be caused by certain interactions between the polymer and the solvent<sup>21,22</sup> or by a combination of liquid–liquid demixing and vitrification.<sup>19,23</sup> A viscosity-related gelation mechanism has been suggested for the membrane-forming system polysulfone (PSF)–dimethylacetamide (DMAC)–water.<sup>1,2</sup> It is, however, difficult to distinguish a gel from a highly concentrated polymer solution, and a clear picture concerning gelation in polymer solutions and its

<sup>®</sup> Abstract published in *Advance ACS Abstracts*, February 15, 1996.

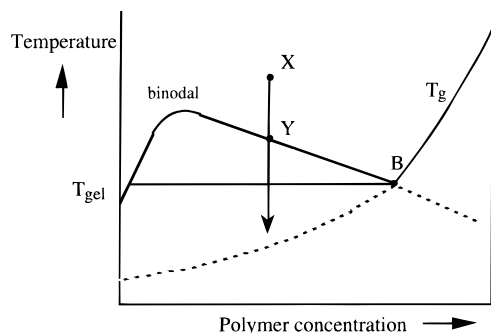


**Figure 1.** Schematic binary phase diagram illustrating the mechanism suggested by Berghmans for the gelation of amorphous polymers.  $T_g$  is the vitrification temperature.  $T_{gel}$  is the gelation temperature. B is Berghmans' point which represents the intersection of the binodal and the vitrification temperature curve.

relevance to membrane formation is still missing.

The aim of this study is to clarify the role of gelation in the structure-forming process of membranes made by immersion precipitation. Based on a mechanism suggested by Berghmans<sup>23</sup> for the gelation of a binary system consisting of an amorphous polymer and a solvent, a mechanism for the gelation of an amorphous polymer in mixtures of a solvent and a nonsolvent is proposed and used to describe the membrane formation process.

### Gelation Mechanism

According to Berghmans,<sup>23</sup> gelation of an amorphous polymer in a solvent results from liquid-liquid phase separation arrested by vitrification of the polymer rich phase. This mechanism is illustrated in Figure 1 which shows the phase diagram of a binary system consisting of an amorphous polymer and a solvent. In the phase diagram the binodal intersects with the vitrification boundary of the system.

If a homogeneous solution of a composition indicated by point X in Figure 1 is cooled down to Y at the binodal, it separates into two phases, i.e., a polymer poor and a polymer rich phase. Upon further cooling the polymer rich phase will reach a composition represented by point B. At this point, the polymer rich phase vitrifies, and the structure of the demixed solution is fixed. If the cooling speed is not infinitely slow, a porous glass will be formed. Such a porous glass is defined by Berghmans as a gel. According to this definition, gelation of amorphous polymer has the following characteristics. 1. Gelation occurs in a system described by a temperature-concentration phase diagram at the intersection of the binodal with the glass transition boundary. 2. The gelation temperature of the polymer-solvent system is constant, independent of the initial concentrations of the polymer solutions. 3. Liquid-liquid demixing is necessary for the formation of a usually turbid gel.

In literature, many systems can be found<sup>19-25</sup> which form gels according to the definition of Berghmans. In certain polymer solutions gelation can occur following a different mechanism<sup>21,22</sup> which requires some sort of complex formation between the polymer and the solvent. This gelation process is rather slow and will most likely be of no relevance for membrane formation by immersion precipitation.

In this paper this concept of gelation will be transferred to a ternary system consisting of an amorphous polymer, a solvent, and a nonsolvent. The gelation

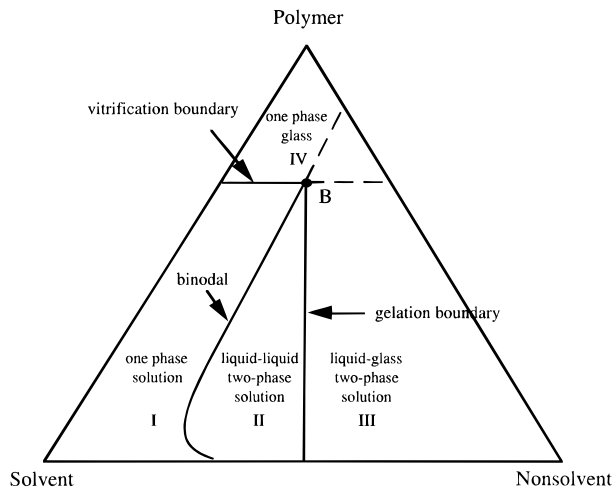


**Figure 2.** Schematic ternary phase diagram used to describe Berghmans mechanism for ternary systems. Solutions in region I are in a homogeneous liquid state. In region II, polymer solutions separate into two liquid phases. Region III is a two-phase glass region consisting of one liquid phase which is the polymer lean phase and one glass phase. Solutions in region IV are in a homogeneous glass state. Point B is referred to as the Berghmans point for a ternary system at a particular temperature.

process was experimentally monitored by measuring the glass transition temperature, which is appropriate for the purpose of our present research. The phase diagram of such a ternary system is shown schematically in Figure 2. The figure indicates that at a given temperature the system can be divided in four distinct regions. Region I represents the homogeneous polymer solution. In region II the solution is separated into two liquid phases, i.e., a polymer lean and a polymer rich phase. In region III the polymer rich phase of a demixed polymer solution has reached its glass state. In region IV the solution is in one phase and has a glass state. This phase diagram will be used later to discuss the membrane formation process by immersion precipitation process.

### Experimental Procedures

**Materials and Their Properties.** The polymers used were poly(ether sulfone) (PES) (5200P; ICI) and polysulfone (PSF) (Udel 3500; Amoco).  $T_g$  of PES as determined by DSC is 225 °C. The solvents *N*-formylpiperidine (FP), dimethyl sulfoxide (DMSO), *N,N*-dimethylacetamide (DMAC), *N*-methylpyrrolidone (NMP), and 2-methyl-2,4-pentanediol (MPD) were purchased from Merck (synthesis grade) and used as received. The  $T_g$ 's of DMSO, DMAC, and water were obtained from literature<sup>26</sup> and are 150, 146, and 137 K, respectively. The  $T_g$ 's of FP and NMP were calculated with an empirically developed equation.<sup>27</sup> The  $T_g$  for FP was calculated to be 144 K and that for NMP to be 143 K.

**Cloud Point Measurements.** Cloud point data were measured by titration. Pure nonsolvent was slowly added to a homogeneous polymer solution at constant temperature until permanent turbidity was detected visually.

Theoretically experimental cloud point data should coincide with calculated binodal or spinodal points. However due to effects such as polydispersity of the polymer sample, this is not necessarily the case. By titration with nonsolvent, spinodal demixing can only occur after crossing the binodal; therefore, spinodal demixing is excluded in our experiments. In this paper the terms 'cloud point' and 'binodal' will be used interchangeably.

**Determination of  $T_g$ : Homogeneous Polymer Solutions.** Differential scanning calorimetry (DSC) measurements were carried out with a liquid-nitrogen-cooled Perkin-Elmer DSC-II apparatus coupled with a Thermal Analysis data

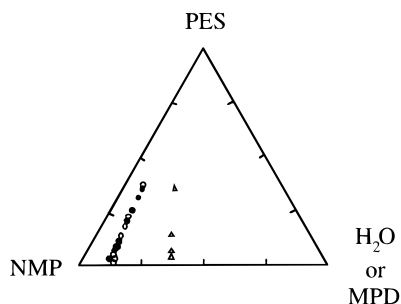


**Figure 3.** Cloud point data for H<sub>2</sub>O–NMP–PES and MPD–NMP–PES systems at 25 °C. (●) cloud point data measured in this study for the H<sub>2</sub>O–NMP–PES system, (○) data from literature<sup>29</sup> for the same system, and (Δ) data measured in this study for the MPD–NMP–PES system.

system (TADS). Indium ( $T_m = 156.6$  °C) was used for calibration. Samples were prepared by placing 40–50 mg of 20 wt % PES solutions into sample pans and evaporating the solvents at 100 °C to the required concentration. The sample pans were then tightly sealed. The sealed pans were stored at 100 °C for at least 1 week before performing DSC measurements. Samples of PES in mixtures of NMP and water were prepared by dissolving the appropriate amount of PES powder and a mixture of NMP/water (9/1, w/w) into the sample pans which were then tightly sealed and annealed at 100 °C for 1 week to ensure homogeneous solutions. All the sealed sample pans were weighed before and after annealing. The homogeneity of the solution could be checked by DSC measurements. For samples with poor homogeneity, the DSC diagrams showed a very broad  $T_g$  signal. Samples that showed poor homogeneity could be improved in their homogeneity by annealing them for ca. 20 min at a temperature of about 60 °C above their approximated  $T_g$ . The glass transition temperature was measured by quenching the solution to –40 °C followed by heating it at a rate of 20 °C/min. The  $T_g$  was recorded as the middle point of the transition curve of the second run.

**Demixed Polymer Solutions.** To determine the glass transition temperature of the polymer rich phase of a demixed polymer solution, PES solutions at various concentrations were stored at 110 °C for 3 weeks. After this period the solutions were cooled down to room temperature at a speed of about 3 °C/min to allow these to demix. The solutions were kept at room temperature for another 3 weeks. The two phases were separated by centrifugation for 1 week. A certain amount (25–35 mg) of the polymer rich phase was placed into DSC sample pans for determining the glass transition temperature. After DSC measurements the sample pans were weighed again to ensure that no leaking occurred.

**Membrane Preparation.** Membranes were cast from polymer solutions of various concentrations with an initial thickness of 200 μm. The solutions were cast on a small glass plate with a dimension of 60 mm × 40 mm × 1 mm. The amount of solution cast on the glass plate was determined by weighing. Highly concentrated polymer solutions were prepared by casting a 20 wt % PES solution on the glass plate followed by evaporation of part of the solvent until the required concentration was reached. The demixing behavior of the polymer solution when immersed into a water bath was followed visually. Delay time measurements were performed according to a procedure described in the literature.<sup>28</sup>

## Results and Discussion

**Cloud Points.** The results of the cloud points obtained for the system H<sub>2</sub>O–NMP–PES at 25 °C shown in Figure 3 are in agreement with literature data.<sup>29</sup> The binodal of the MPD–NMP–PES system, also shown in Figure 3, is located closer to the nonsolvent corner compared to the binodal of the H<sub>2</sub>O–NMP–PES system. The results are well in agreement with calculated data given in the literature<sup>28</sup> which postulate for a small polymer–nonsolvent interaction parameter

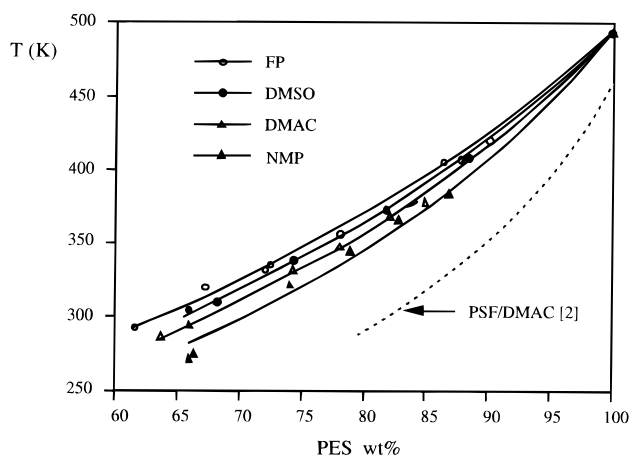


**Figure 4.**  $T_g$  depression of PES by various solvents. The dashed curve represents the  $T_g$  depression of PSF by DMAC.<sup>2</sup>

(i.e., a rather mild interaction) or a large solvent–nonsolvent interaction parameter, a binodal is located close to the polymer–nonsolvent axis.

**Glass Transition Temperature Depression of PES: By Different Solvents.** Samples of PES in NMP were examined with DSC, at concentrations from 40 to 85 wt %. For solutions with PES concentrations smaller than 50 wt %, no transition signals were detected in the experimental range of –40 to 150 °C. From the DSC experiments it can be concluded that no crystallization or local ordering existed in the PES–NMP solutions.

Wijmans<sup>1</sup> demonstrated that for the system H<sub>2</sub>O–DMAC–PSF the DSC measurements of a highly concentrated PSF solution showed a melting peak near the melting temperature of DMAC. This behavior of the solution was not observed in this study with homogeneous solution samples. It is believed that the melting peak observed in Wijmans experiments was due to the sample preparation method: The highly concentrated polymer solution was prepared by separation of the polymer rich phase from a demixed polymer solution. In the current experiments it was very difficult to separate a demixed polymer solution with a polymer rich phase of relatively high polymer concentration completely into two phases by centrifugation. Usually, a small amount of the polymer lean phase was trapped in the polymer rich phase. This was indicated by the fact that the polymer rich phase remained turbid even after a long time of centrifugation. So, the polymer solution used by Wijmans might not have been homogeneous, and the observed melting peak could be that of the trapped polymer lean phase, which is in the exact same position.

Figure 4 shows the  $T_g$  depression of PES by FP, DMSO, DMAC, and NMP. It can be seen that among the solvents, the  $T_g$  of PES is depressed most strongly by NMP. The  $T_g$  depression of PES by the different solvents is decreasing in the sequence of NMP > DMAC > DMSO > FP. The  $T_g$  depression of membrane-forming systems can be described quite well by the following relation:<sup>16,2,27</sup>

$$T_g = \frac{R\phi_2 T_{g2} + \phi_3 T_{g3}}{R\phi_2 + \phi_3} \quad (1)$$

The subscripts 2 and 3 in the equation denote the solvent and the polymer, respectively.  $\phi_i$  is the volume fraction of component  $i$ , and  $T_{gi}$  is the glass transition

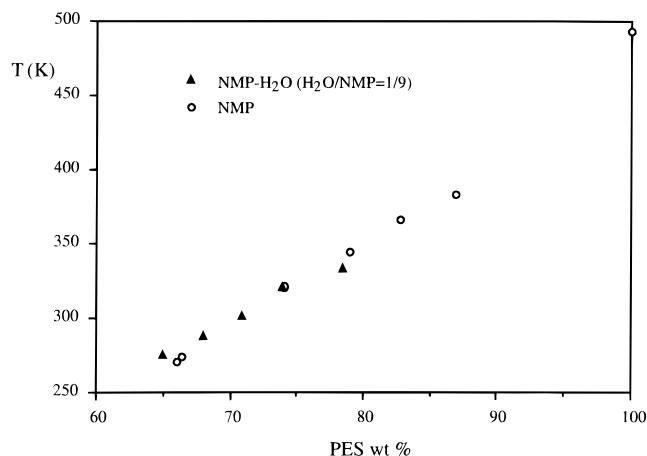


**Figure 5.** Comparison of  $T_g$  depression of PES by pure NMP and a mixture of NMP and water (9/1).

**Table 1.** Kelley–Bueche Parameter  $R$ <sup>30</sup> for the  $T_g$  Depression of PES by Various Solvents Together with the PES Concentration Related to  $T_g$  at 298 K

solvent	$R$	PES concentration (wt %) at $T_g = 298$ K
FP	2.21	63
DMSO	2.45	64
DMAC	2.62	67
NMP	2.98	70

temperature of component  $i$ .  $R$  is related to the thermal expansion coefficients of the different components<sup>30</sup> but is often treated as a fitting parameter.<sup>2,16</sup>

Equation 1 was used to describe the  $T_g$  depression of PES by the various solvents. The fitting parameter  $R$  for the various solvents and the polymer concentration when the  $T_g$  was 298 K is shown in Table 1.  $T_g$  depression data given in the literature<sup>2</sup> for PSF by DMAC show that for this system the  $T_g$  at 298 K is reached when the PSF concentration was 82 wt %, which is much higher than the 67 wt % obtained for PES in DMAC.

**By a Mixture of NMP and Water.** Samples of homogeneous solution of PES in mixtures of NMP and water were prepared by placing the appropriate amounts of PES powder, NMP, and water into DSC sample pans which were then kept at elevated temperature for a certain time.

Figure 5 shows the  $T_g$  depression behavior of PES by a mixture of NMP and water with a ratio of 9/1. The results indicate that the  $T_g$  depression of PES by a mixture of NMP and water is in the same order as by pure NMP which is not expected since the interactions between PES–NMP and PES–water are significantly different. However, the amount of water added to the polymer solution was quite limited, which might be the reason why no difference was found between the  $T_g$  depression of PES by pure NMP and by a mixture of water and NMP.

According to the cloud point data shown in Figure 3, very little water can be tolerated for the system to stay in the homogeneous region. For homogeneous polymer solutions with >60 wt % PES, the water concentrations are <6 wt %. From the results shown in Figure 5 and the cloud point data shown in Figure 3, it can be concluded that in the homogeneous region the  $T_g$  depression of PES by mixtures of NMP and water is about the same as that obtained by pure NMP. Extending the relation expressed in eq 1 to ternary systems<sup>2</sup> shows that the effect of adding a nonsolvent to a

**Table 2.** Glass Transition Temperatures and PES Concentrations of the Polymer Rich Phase of Demixed Polymer Solutions of 10 wt % PES and Various NMP/Water Ratios

water concn of demixed solution (wt %)	$T_g$ (°C)	polymer concn of polymer rich phase (wt %) <sup>a</sup>
20	20.5	58
22	27.2	55
24	30.5	53
26	38.0	49
30	60.0	40

<sup>a</sup> Underestimated values, see text.

polymer solution is very low. This means that the vitrification boundary is nearly parallel to the solvent–nonsolvent axis of the related ternary phase diagram, i.e., the  $T_g$  depression of the polymer by the solvent is nearly the same as by mixtures of the solvent and the nonsolvent.

**Determination of the Gelation Boundary.** As indicated in Figures 1 and 2, the gelation boundary of amorphous polymers is a specific tie line whose polymer rich phase concentration is located at the intersection of the binodal with the  $T_g$  curve. For a ternary system at a temperature of 298 K, this tie line can be determined by separating and analyzing the two equilibrium phases for their composition. However, it is extremely difficult to separate the demixed polymer solution completely when the polymer concentration of the polymer rich phase is relatively high. The gelation boundary can be measured in a different way. First, the intersection point of the binodal and the vitrification boundary is obtained from cloud point and vitrification data. Then, knowing the overall composition of a demixed polymer solution with a polymer rich phase whose  $T_g$  is at the desired temperature, the gelation boundary can be obtained by simple mass balance assuming that the two phases of the demixed polymer solution are in equilibrium.

In this study, a series of demixed polymer solutions were prepared by using a constant polymer concentration (10 wt %) and varying the ratio of water to NMP. The glass transition temperatures of the polymer rich phase of the demixed solutions were measured. The PES concentrations of the polymer rich phase were also determined by complete evaporation of NMP and water. Table 2 gives the results of these measurements.

From the data shown in Table 2, the overall water concentration of the demixed polymer solution with a  $T_g$  is 25 °C if its polymer rich phase can be interpolated to be about 21.5 wt %. The related PES concentration of the polymer rich phase determined by complete evaporation of NMP and water is about 56 wt %, which is much lower than the PES concentration at Berghmans point which is ca. 70 wt %. The discrepancy is caused by underestimating of the PES concentrations shown in Table 2 due to trapped polymer lean phase in the polymer rich phase which could not be removed from the polymer rich phase by centrifugation.

The DSC measurements of the polymer rich phase samples showed a peak near the melting point of NMP. As expected a higher amount of water in the polymer solution resulted in a higher glass transition temperature of the polymer rich phase. Due to random trapping of polymer lean phase, decrease of the polymer concentration of the polymer rich phase with increase of the water concentration in the solution might simply be an experimental coincidence. In principle the polymer

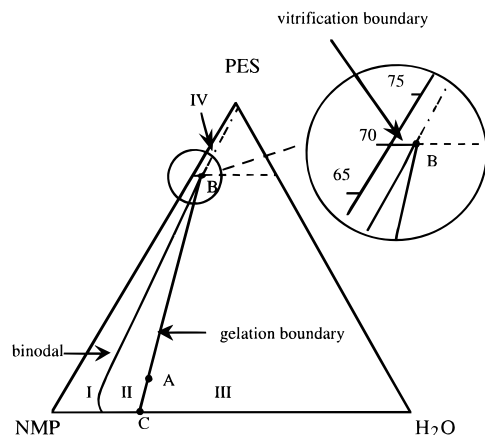


**Figure 6.** Ternary phase diagram of the system  $\text{H}_2\text{O}$ –NMP–PES at 25 °C. Point A in the figure represents the overall composition of a demixed polymer solution with 10 wt % PES and 21.5 wt % water in NMP. The  $T_g$  of the polymer rich phase of this demixed solution is 25 °C. There are four regions in the diagram. The definition of the four regions is given in Figure 2. Point B is the so-called Berghmans point, i.e., the point of vitrification of the polymer rich phase of the separated mixture represented by point A. Point C is the intersection point of the gelation boundary with the binodal which is approximately identical with the solvent–nonsolvent axis and has a composition of 76/24 NMP/water (w/w). It represents the polymer lean phase of the separated mixture.

concentration of the polymer rich phase should increase with increase of the water concentration in the demixed solution.

**Ternary Phase Diagram of the System  $\text{H}_2\text{O}$ –NMP–PES.** The ternary phase diagram of the system  $\text{H}_2\text{O}$ –NMP–PES at 25 °C generated from the above data is shown in Figure 6. Figure 6 shows that the vitrification boundary of the  $\text{H}_2\text{O}$ –NMP–PES system intersects the binodal, which means that the gelation mechanism postulated by Berghmans for solutions of amorphous polymers holds for this system. The phase diagram indicates three boundaries, i.e., a binodal, a vitrification, and a gelation boundary. The three boundaries divide the system into four regions as shown in Figure 2. Region I is a one-phase liquid. Region II is a two-phase liquid, i.e., the region where liquid–liquid demixing occurs. Region III is a two-phase glass region. Within this region a liquid polymer lean phase is in equilibrium with vitrified, i.e., solid, polymer. Region IV is a one-phase glass region. Liquid–liquid demixing cannot take place within this region. This is demonstrated experimentally later.

Point C in Figure 6 is the point where the gelation boundary intersects with the binodal which in this case is approximately identical with the solvent–nonsolvent axis. The composition of this point obtained by extrapolation is 76/24 NMP/water (w/w). Point C represents the maximum solvent concentration that can be tolerated in a coagulation bath to prepare a solidified membrane. This means that a NMP concentration higher than 76 wt % in the coagulation bath will not give a solid membrane structure since the polymer concentration of the polymer rich phase will be lower than the vitrification concentration.

**Examination of the Gelation Boundary.** As described previously, the extension of the gelation mechanism for binary solutions of amorphous polymers to ternary systems consisting of a polymer, a solvent, and a nonsolvent leads to the definition of point C in Figure 6 which defines the maximum solvent concentration in the coagulation bath that can be used to obtain a

**Table 3.** Elongation of Membranes Formed from a Polymer Solution of 30 wt % PES and 6 wt % Water in NMP Immersed into Coagulation Baths with Various NMP Concentrations

NMP concn in coagulation bath (wt %)	elongation of the film ( $L/L_0$ ) <sup>a</sup>
0	1
60	1
65	1
70	1
75	1
77.5	
80	∞

<sup>a</sup>  $L_0$  is the initial film length and  $L$  the final film length.

**Table 4.** Demixing Behavior of Highly Concentrated Polymer Solutions in the Water Bath

polymer solution	demixing behavior in water
30 wt % PES in NMP	instantaneous demixing
62 wt % PES in NMP	instantaneous demixing
65 wt % PES in NMP	instantaneous demixing
72 wt % PES in NMP	no demixing (no turbidity)
74 wt % PES in NMP	no demixing (no turbidity)
30 wt % PSF in DMAC	instantaneous demixing
60 wt % PSF in DMAC	instantaneous demixing

solidified membrane. For the system  $\text{H}_2\text{O}$ –NMP–PES, this point has been determined by cloud point and DSC measurements. It has also been confirmed by membrane-casting experiments.

Membranes were cast from a polymer solution of 30 wt % PES and 6 wt % water in NMP immersed in coagulation bath with different NMP concentrations. The cast films were kept in the coagulation bath for 2 days. Then a sample 100 mm × 10 mm was cut, and its elongation was measured by hanging a weight of 35 g at the film. The results are given in Table 3.

It was found that prepared by precipitation bath with a NMP concentration  $\geq 77.5$  wt %, the films were broken immediately in the elongation test. NMP concentrations of  $<75$  wt % in precipitation bath gave films which exhibited no elongation under the same test conditions. This experiment confirmed that for this system vitrification is responsible for fixation of the membrane structures. From the elongation test, the maximum NMP concentration in the coagulation bath that still leads to a solid membrane was determined to be between 75 and 77.5 wt %. This is in good agreement with the data obtained from Figure 6 which indicate that the method used to determine the gelation boundary is quite reliable.

**Demixing Behavior in Relation to Vitrification Phenomenon.** The demixing behavior of solutions of PES in NMP and PSF in DMAC immersed into a water bath was studied. The results are shown in Table 4. Table 4 shows that for polymer solutions with PES concentrations  $\leq 65$  wt % instantaneous demixing took place when the solutions were immersed into a water bath. For solutions with PES concentration  $>72$  wt % no demixing occurred. From Figure 6 it can be seen that at concentrations in excess of 70 wt % PES in NMP, the solution is in a glass state at room temperature. From Figure 6 with the experimental observations shown in Table 4, it becomes evident that instantaneous demixing takes place in a PES solution immersed into water only when the initial polymer solution is in a liquid state. No liquid–liquid demixing can occur in a solution which is in a glass state. The experimental results presented in Table 4 show that liquid–liquid demixing will not be hindered by the high viscosity of a

**Table 5. Weight of a Polymer Film Prepared from a Solution of 74 wt % PES in NMP, Measured before and after Immersion into a Water Bath for 2 h**

before immersion	after immersion
51 mg	46 mg

**Table 6. Demixing Behavior of PES–NMP Solutions in the MPD Bath**

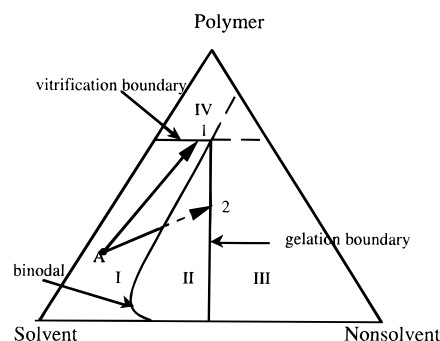
polymer solution	demixing behavior in MPD
20 wt % PES in NMP	delayed demixing
30 wt % PES in NMP	no demixing
40 wt % PES in NMP	no demixing

highly concentrated polymer solution. It will only be excluded when the polymer concentration in the casting solution is higher than the vitrification concentration of the system. Data from ref 2 for the system PSF–DMAC–H<sub>2</sub>O show that the solution is in a liquid state at room temperature when the polymer concentration is <82 wt %. This explains why instantaneous demixing was observed when a polymer solution of 60 wt % PSF in DMAC, which is in accordance with refs 1 and 2, located between the vitrification boundary and the "gelation" boundary is immersed into a water bath. The definition of the gelation boundary in terms of a viscosity boundary as given in ref 2 is somewhat questionable in terms of its practical value since the demixing behavior of such a "gel" does not show any difference compared to the demixing behavior of a "normal" solution when immersed into a water bath, i.e., instantaneous demixing can still take place in the "gel".

In another experiment the weight of a film made out of a 74 wt % PES in NMP solution was measured before and after immersion. The immersion time was 2 h. The result is shown in Table 5. It can be seen that after immersion the weight of the film decreased, although the film remained transparent. This experiment indicates that even though no liquid–liquid demixing could occur in a vitrified polymer solution, the exchange of solvent and nonsolvent between the solution and the coagulation bath does take place. The result of the exchange was that the loss of solvent from the polymer solution was higher than the uptake of nonsolvent by the polymer solution which gave rise to the densification of the final film.

The demixing behavior of PES–NMP solutions in a MPD bath is shown in Table 6. All the polymer solutions presented in this table are in a liquid state. It was found, however, that for PES concentrations >30 wt % no liquid–liquid demixing occurs when immersed into a MPD coagulation bath, and a stiff and transparent film was obtained. The explanation for these observations is that for polymer solutions with PES concentration >30 wt %, the composition path of the system during immersion in the MPD bath crosses the vitrification boundary before traversing the binodal. For polymer solutions with a lower PES concentration (<20 wt %), liquid–liquid demixing of the solution was observed.

**Membrane Formation.** The experimental results obtained for the system H<sub>2</sub>O–NMP–PES and literature data for the system H<sub>2</sub>O–DMAC–PSF<sup>1,2</sup> show at least for these systems that the mechanism suggested by Berghmans for the gelation of amorphous polymers can be used to rationalize the membrane formation during nonsolvent precipitation. The concept can be applied to all polymer–solvent–nonsolvent systems<sup>25</sup> in which the binodal intersects the vitrification boundary. For semicrystalline polymer systems, crystallization may

**Figure 7.** Generalized ternary phase diagram used to describe the membrane formation mechanism. Point A is the initial casting solution composition. The arrows 1 and 2 represent two possible composition paths when a polymer film with composition A is immersed into a nonsolvent bath. The definition of the four regions (I–IV) are shown in Figure 2.

also induce the formation of a gel. However, the time scale of a membrane formation process is in the range of seconds or less and thus much too short for crystallization to have any significant effect. From these outlined considerations, it becomes evident that the gelation mechanism suggested by Berghmans is dominating the membrane structure-forming process. If phase separation in a system is induced by the replacement of a solvent in the polymer solution by a nonsolvent, a large number of nuclei are formed initially by the polymer lean phase. This is followed by coalescence of the nuclei in an attempt to reach a macroscopic two-phase final state. Vitrification of a demixed solution hinders the separation process, and the demixing process is frozen. The final porosity of a membrane is determined by the overall composition of the system at the moment of vitrification. The lever rule can be applied to determine the relative amounts of the polymer rich solid and the polymer lean liquid phase. To obtain a useful membrane, both phases must be continuous. The continuity of the phase is related to the overall composition and the stage of demixing during which vitrification appears. For binary systems<sup>19</sup> it has been shown that the cease of demixing by vitrification at an earlier stage results in a better interconnected porous structure than when vitrification appears at a later stage of demixing.

The above statements can be illustrated with a schematic three-component phase diagram as shown in Figure 7. Point A represents the initial composition of a casting solution. The arrows 1 and 2 represent two possible composition paths when a polymer film with composition A is immersed into a nonsolvent bath. During path 1 the polymer solution undergoes a glass transition, and consequently the solution becomes a homogeneous, dense glass; no gelation takes place. The resulting membrane will show, e.g., for gas separation, the intrinsic polymer transport properties. For path 2 gelation determines the formation of the membrane. Liquid–liquid demixing starts when the path crosses the binodal and will continue as long as the composition path remains in region II. The time associated with the dotted part of path 2 determines when vitrification begins after demixing has started. This time can be defined as *gelation time*.

The area of region II is determined by both the binodal and the gelation boundary. When the area is small it means that after demixing only a small amount of nonsolvent diffusing into the polymer solution is sufficient to induce vitrification, and the gelation time

is short. For the system H<sub>2</sub>O–NMP–PES, this region is rather small and characterized by a very steep gelation boundary as shown in Figure 6. Experiments have shown that membranes prepared from this system vitrified very quickly. It appears that, because the gelation boundary is just a specific tie line, knowledge about the tie line in relation to the thermodynamic properties of the system is also of great importance for the structure formation of a membrane. The composition path shifts with time, while the precipitation front moves into the polymer solution during immersion into the nonsolvent bath.<sup>28</sup> Thus, path 1 in Figure 7 may represent more likely the skin and path 2 the sublayer formation because the ratio of solvent outflow and nonsolvent inflow is higher for the skin formation than for the sublayer. If so, the resulting membrane will show a homogeneous, dense, glassy skin and a porous sublayer.

## Conclusions

The gelation mechanism as defined by Berghmans for a binary solution of an amorphous polymer can be extended to ternary membrane forming systems consisting of a polymer, a solvent, and a nonsolvent. Based on this mechanism, the gelation boundary is defined as a specific tie line whose polymer rich phase concentration is located at so-called Berghmans' point which is given by the intersection of the binodal with the vitrification boundary. The gelation boundary of a ternary system can be determined by cloud point and vitrification measurements of homogeneous solutions as well as of demixed solutions.

In the phase diagram of the system H<sub>2</sub>O–NMP–PES at 25 °C, which was determined experimentally, four different regions can be distinguished as follows: (I) a homogeneous liquid region, (II) a two-phase region with two liquid phases in equilibrium, (III) a two-phase region with a liquid and a glass phase in equilibrium, and (IV) a homogeneous glass region.

Membrane-casting experiments with the systems H<sub>2</sub>O–NMP–PES and H<sub>2</sub>O–DMAC–PSF showed that vitrification of the polymer is responsible for the fixation of the membrane structure. Liquid–liquid demixing of these systems can only be prevented by vitrification when polymer concentration in the solution is higher than that determined by vitrification boundary.

It has been demonstrated experimentally that the skin of a membrane made by immersion precipitation can be formed by vitrification without the system undergoing liquid–liquid demixing. For the system

MPD–NMP–PES, the formation of membranes can even be completely dominated by vitrification without liquid–liquid demixing taking place.

## References and Notes

- (1) Wijmans, J. G.; Kant, J.; Mulder, M. H. V.; Smolders, C. A. *Polymer* **1985**, *26*, 1539.
- (2) Gaides, G. E.; McHugh, A. J. *Polymer* **1989**, *30*, 2118.
- (3) Broens, L.; Altena, F. W.; Smolders, C. A.; Koenhen, D. M. *Desalination* **1980**, *32*, 33.
- (4) Callister, S.; Keller, A.; Hikmet, R. M. *Makromol. Chem., Macromol. Symp.* **1990**, *39*, 19.
- (5) Muhr, A. H.; Blanshard, J. M. V. *Polymer* **1982**, *23*, 1012.
- (6) Tanaka, F. *Macromolecules* **1990**, *23*, 3784.
- (7) Tanaka, F. *Macromolecules* **1990**, *23*, 3790.
- (8) Tanaka, F.; Stockmayer, W. H. *Macromolecules* **1994**, *27*, 3943.
- (9) Hikmet, R. M.; Callister, S.; Keller, A. *Polymer* **1988**, *29*, 1378.
- (10) Guenet, J.-M. In *Handbook of polymer science and technology*; Cheremisinoff, N. P., Ed.; Marcel Dekker Inc.: New York, 1989; Vol. 1.
- (11) Keller, A. In *Structure-property relationships of polymer solids*; Hiltner, A., Ed.; Plenum Press: New York, 1983.
- (12) Guenet, J.-M.; Lotz, B.; Wittmann, J.-C. *Macromolecules* **1985**, *18*, 420.
- (13) Domszy, R. C.; Alamo, R.; Edwards, C. O.; Mandelkern, L. *Macromolecules* **1986**, *19*, 310.
- (14) Mulder, M. H. V. *Basic principles of membrane technology*; Kluwer Academic Publishers: Dordrecht, The Netherlands, 1991.
- (15) Matsuo, E. S.; Orkisz, M.; Sun, S. T.; Li, Y.; Tanaka, T. *Macromolecules* **1994**, *27*, 6791.
- (16) Burghardt, W. R.; Yilmaz, L.; McHugh, A. J. *Polymer* **1987**, *28*, 2085.
- (17) Kesting, R. E. *Synthetic polymeric membranes—a structure perspective*, 2nd ed.; John Wiley and Sons: New York, 1985.
- (18) Yang, Y. C.; Geil, P. H. *J. Macromol. Sci. Phys.* **1983**, *B22*, 463.
- (19) Schneider, T.; Wolf, B. A.; Kasten, H.; Kremer, F. *Macromolecules* **1991**, *24*, 5387.
- (20) Tan, M.-M.; Moet, A.; Hiltner, A.; Baer, E. *Macromolecules* **1983**, *16*, 28.
- (21) Francois, J.; Gan, J. Y. S.; Guenet, J.-M. *Macromolecules* **1986**, *19*, 2755.
- (22) Guenet, J.-M.; Klein, M.; Menelle, A. *Macromolecules* **1989**, *22*, 493.
- (23) Arnauts, J.; Berghmans, H. *Polym. Commun.* **1987**, *28*, 66.
- (24) Tsai, F.-J.; Torkelson, J. M. *Macromolecules* **1990**, *23*, 775.
- (25) Vandeweerdt, P.; Berghmans, H.; Tervoort, Y. *Macromolecules* **1991**, *24*, 3547.
- (26) Fedors, R. F. *J. Polym. Sci., Polym. Lett. Ed.* **1979**, *17*, 719.
- (27) Li, S.-G. Ph.D. Thesis, University of Twente, The Netherlands, 1994.
- (28) Reuvers, A. J.; Smolders, C. A. *J. Membr. Sci.* **1987**, *34*, 67.
- (29) Zeman, L.; Tkacik, G. *J. Membr. Sci.* **1988**, *36*, 119.
- (30) Kelley, F. N.; Bueche, F. *J. Polym. Sci.* **1961**, *50*, 549.

MA9508966